C.P. No. 776

MINISTRY OF AVIATION

AERONAUTICAL RESEARCH COUNCIL

CURRENT PAPERS

Bow-Shock Establishment and Stagnation-Point Pressure Measurements for a Blunt-Nosed Body at Supersonic Speeds

By

L Davies

LONDON: HER MAJESTY'S STATIONERY OFFICE

1965

Price 4s. 6d. net

C.P. No.776

Bow-Shock Establishment and Stagnation-Point Pressure Measurements for a Blunt-Nosed Body at Supersonic Speeds

- By -
L. Davies

April, 1964

SUMMARY

A shock tube study has been made of the bow shock establishment process in air and the pressure time profiles at the stagnation point of a blunt-nosed body in air, oxygen and argon during the establishment of supersonic flow conditions over the body. The incident shock Mach number range was $M_S = 2 \rightarrow 8$ giving a flow Mach number range behind the primary shock of $M_2 = 1 \rightarrow 2{\cdot}08$. A simple theoretical description of the establishment process is seen to agree closely with the experimental measurements of the bow shock position along the stagnation streamline during bow shock formation.

Contents

4./

Replaces N.P.L. Aero. Report No.1098 - A.R.C.25 794.
Published with the permission of the Director National Physical Laboratory.

Nomenclature

a	velocity of sound
H	enthalpy
M	Mach number
P_{ij}	pressure ratio = p_i/p_j
p	pressure
r	body diameter
s	distance measured along the stagnation streamline from the stagnation point
t	time
t^*	bow shock establishment time
u	stream velocity
w	shock velocity
α	$\frac{\gamma + 1}{\gamma - 1}$
γ	specific heat ratio
δ	bow shock detachment distance
ρ	density

Subscripts

1	initial conditions in the channel of the shock tube
2	conditions between the primary shock and the contact surface
t	stagnation conditions
R	reflected shock
s	refers to primary shock Mach number

1./

1. Introduction

A knowledge of the flow conditions over a body in supersonic flight is important in the design of high-speed aircraft. The pitot tube is a well-established instrument for the measurement of stagnation pressure of the freestream from which, by substituting the pressure (for supersonic flow) in the Rayleigh supersonic pitot formula, the flow Mach number may be computed.

As the flow establishes over a blunt-nosed body in a shock tube, immediately subsequent to the passage of the primary shock wave, the flow parameters at the stagnation point vary in times which are very short compared with the response time of the pitot tube (~ 1 ms) but acceptable to the bar gauge[3] (response time ~ 3 microseconds).

Measurement of the pressure variation during the establishment of the bow shock wave in supersonic flow will aid the theoretical investigation of the establishment process, whilst the quasi-equilibrium stagnation pressure measurements will add to the data on the hot flow behind the primary shock, and the stagnation point conditions of a body in supersonic flight.

In view of the fast response of the bar gauge and its accuracy under fast loading rates, it was considered that if suitably mounted, useful measurements of the quasi-steady-state stagnation pressure, and the time taken to achieve this value, could be made using this gauge. A piezo-electric element has been used in a stagnation-point pressure probe by Filler[1] (1960) whilst studying the pressures arising from the passage of spherically expanding blast waves. However, the gauge design is completely different and the circumstances dissimilar to those in the present investigation.

In conjunction with the pressure measurements a photographic investigation of the formation of the bow shock wave shows that the concept of a constantly decelerating shock wave closely predicts the position of the bow shock wave along the stagnation streamline during the bow-shock establishment process.

2. Theory

The Rayleigh supersonic pitot formula for an ideal gas is

$$\frac{p_2}{p_t} = \frac{\left[\frac{2\gamma}{\gamma+1} M_2^2 - \frac{\gamma-1}{\gamma+1}\right]^{\frac{1}{\gamma-1}}}{\left[\frac{\gamma+1}{2} M_2^2\right]^{\frac{\gamma}{\gamma-1}}} . \qquad \ldots (1)$$

Stollery[2] has found that large deviations from ideal values are obtained when real gas effects are considered. He obtains the conditions behind the normal shock by solving, graphically, the equation

$$H_2 - H_1 = \tfrac{1}{2}(p_2 - p_1)\left[\frac{1}{\rho_2} + \frac{1}{\rho_1}\right] \qquad \ldots (2)$$

giving/

4. Analysis of Results

With regard to the higher than ideal stagnation pressures deduced from the level portion C - D in the records, Stollery has shown that real gas effects (which included dissociation and ionization) have a strong influence on the value of the stagnation pressure in the region behind the normal shock wave, real gas effects are increasingly important for $M_s > 3$, and for $M_s > 6$ ideal-gas results are considered[2] of little value. The increase in stagnation pressures is due to the fact that (i) more energy is needed to produce a given primary-shock Mach number in real air than in a perfect gas and (ii) a larger density than ideal is obtained in the real-gas case. The low pressures obtained using argon are due to the absence of, for example, vibration relaxation and dissociation effects.

For the lower values of M_s the initial 50 microseconds of the pressure traces are occupied by the variation in stagnation pressure as the bow shock wave establishes. With increasing M_s this pressure dip becomes shallower disappearing at $M_s = 6$. At the same time the duration of the dip lessens. Calculations suggest that for $M_s > 6$ the flow conditions equilibrate in times which cannot be resolved using the bar gauge (i.e., ≤ 3 microseconds).

A simple bow-shock development model is proposed (shown in Fig.6). In Fig.6.1 the initial condition is shown where the primary shock wave approaches the body. Fig.6.2 shows a simplified picture of the situation immediately subsequent to primary shock-wave impingement where a small section in the middle of the primary shock wave has reflected. The reflected shock is decelerated, until it comes to rest in the bow shock wave detachment distance (Fig.6.3). A uniform deceleration is assumed for the purposes of a simple calculation. This deceleration occurs as a result of the mass flow out of the region between the rejected portion of the primary shock wave and the nose of the body, around the shoulders of the body.

From the continuity equations, the reflected shock velocity is given by

$$w_R = a_1 \frac{[2 + (\alpha_1 - 1) P_{12}]}{[(\alpha_1 + 1) P_{12} (\alpha_1 + P_{12})]^{\frac{1}{2}}} .$$

If the shock detachment distance in the flow behind the primary shock is δ then from the simple equations of motion assuming a constant retarding force, the time taken for the small reflected shock to stop in this bow-shock detachment distance is

$$t^* = 2 \frac{\delta}{a_1} \frac{[(\alpha_1 + 1) P_{12} (\alpha_1 + P_{12})]^{\frac{1}{2}}}{[2 + (\alpha_1 - 1) P_{12}]} .$$

δ is obtained for air from a graph drawn (using data supplied by Li and Geiger, Hayes and Marsden and Moeckel) and discussed by A. J. Vitale et al[6]. Reflected shock velocities for real-gas cases are obtained from data published by Bernstein[7]. Using this data, calculations for two cases in air at $M_s = 3$, 6 and $p_1 = 10$ cm and 10 mm respectively yield the result that

t*/

$t^* = 16$ microseconds for $M_s = 3$ and $t^* = 3{\cdot}3$ microseconds for $M_s = 6$. This is in complete agreement with the experimentally obtained pressure time profiles from an examination of which it was considered that the bow shock wave should be formed after the reflected shock has decelerated to rest relative to the tube walls, the pressure decaying during this process. It was also considered that the rest of the dip formation is a result of relaxation phenomena. As far as the pressure-time profile is concerned, the effect of relaxation phenomena on the pressure occurs immediately subsequent to the primary shock impingement. The dominant factor is the deceleration of the small reflected shock wave. Until this effect ceases the pressure will decay. Thereafter the pressure will follow the relaxation phenomena assuming that the relaxation time is greater than the bow-shock establishment time and no other flow perturbations exist. During the whole of this time the flow will be unsteady. The bow-shock detachment-distance will vary slightly after the deceleration to rest of the small reflected portion of the primary shock, due to these relaxation phenomena.

Comparison of the three profiles obtained in air, oxygen, and argon (Fig.7) emphasises the dependence of the rise B-C on relaxation effects. Whereas in the case of air and oxygen there is a definite A-B-C profile, in the case of argon the pressure falls to and remains at the point B level (see Fig.7).

Owing to the limitations of the apparatus, in order to increase the Mach number of the primary shock wave the value of the initial pressure was decreased, and resulted in absolute values of stagnation pressure remaining at approximately the same magnitude (200 - 300 cms Hg). This is very important since it implies that the results presented here are not dependent on the absolute pressure, but depend merely on the flow velocity.

5. Photographic Investigation

Schlieren photographs were taken in the N.P.L. 6 in. × $3\frac{1}{2}$ in. shock tube[8] using an identical $\frac{1}{2}$ in. blunt-nosed cylinder to that employed for the pressure measurements, and also a 7/32 in. diameter model. This tube has a 3 ft long driver and 12 ft working section. Single shots were taken at varying delays after the initiation of bow-wave reflection at the same primary shock Mach number. Since the theory predicts, and it may also be concluded intuitively, that the bow shock establishment process takes longer at lower primary shock Mach numbers a Mach number of 2·23 was chosen using nitrogen as driver and air as driven gas. The flow behind the primary shock wave is then just supersonic ($M_2 = 1{\cdot}076$). This gives a longer time interval in which to examine the establishment process and shock profile.

Measurements made from the series of photographs taken with the $\frac{1}{2}$ in. and 7/32 in. bars respectively are shown in Fig.8(a) and Fig.8(b) and a composite diagram of the bow shock at various times during the establishment process shown in Fig.9. Using the equations of motion the relation between the time taken for the bow shock to reach a distance 'S' along the stagnation streamline assuming constant deceleration (as in Section 4) is given by

$$t = \frac{2\delta}{w_R}\left(1 - \left(1 - \frac{s}{\delta}\right)^{\frac{1}{2}}\right)$$

or/

or $$t = t^* \left(1 - \left(1 - \frac{s}{\delta}\right)^{\frac{1}{2}}\right) .$$

Even though the deceleration may not be constant the answer should be of the same order of magnitude as the experimental value. Indeed the agreement between this very simple theory and actual experiment is good, as is shown in Fig.8 when using real-gas values for w_R.

Given the bow-shock detachment distance for a blunt-nosed body, this simple theory closely predicts the bow shock position at any time during the establishment process and the establishment time.

Photographs of the bow shock establishing at the nose of the $\frac{1}{2}$ in. and 7/32 in. bodies are shown in Figs.10(a) and (b).

6. Conclusions

The variation of stagnation point pressure with Mach number for the real gas case as predicted by Stollery has been shown to occur in air and oxygen, for $M_s = 3 - 6$. The argon results agree more closely with theory, the situation expected using a monatomic gas. Values above $M_s = 6$ in air and oxygen were not used since the pressure increased continuously over the first 100 microseconds of recording time. During the establishment of the bow shock wave a dip in pressure occurs associated with the reflection of a section in the middle of the primary shock wave as it encounters the gauge, and relaxation phenomena behind the bow shock wave.

Photographic evidence agrees with the predictions from the pressure measurements and shows that this simplified theoretical approach can closely predict the bow shock establishment time and the position of the bow shock wave during the establishment process.

Acknowledgment

Part of this work was carried out whilst a D.S.I.R. Research Student. I am indebted to Dr. D. H. Edwards (U.C.W. Aberystwyth) and Dr. L. Pennelegion (N.P.L.) for advice and encouragement and to Mr. M. J. Larcombe for taking the schlieren photographs.

References/

References

No.	Author(s)	Title, etc.
1	W. S. Filler	Jr. Phys. Fluids, 3, No.2 (1960).
2	J. L. Stollery	Real gas effects on shock-tube performance at high shock strengths. A.R.C. C.P.No.403. November, 1957
3	D. H. Edwards	J. Sci. Instr., 35, 346 (1958).
4	J. C. Breeze	Ph.D. Thesis, University of Wales.
5	D. H. Edwards, L. Davies and R. Lawrence	To be published.
6	A. J. Vitale, N. S. Diaconis, E. M. Kaegi and W. R. Warren	G. E. C. Missile & Ordnance Systems Dept. Document No.58SD214 (1958).
7	L. Bernstein	Tabulated solutions of the equilibrium gas properties behind the incident and reflected normal shock-wave in a shock-tube. I. Nitrogen. II. Oxygen. A.R.C. C.P. No.626. April, 1961.
8	D. W. Holder, C. M. Stuart and R. J. North	The interaction of a reflected shock with the contact surface and boundary layer in a shock tube. A.R.C.22 891. September, 1961.

DR
DH

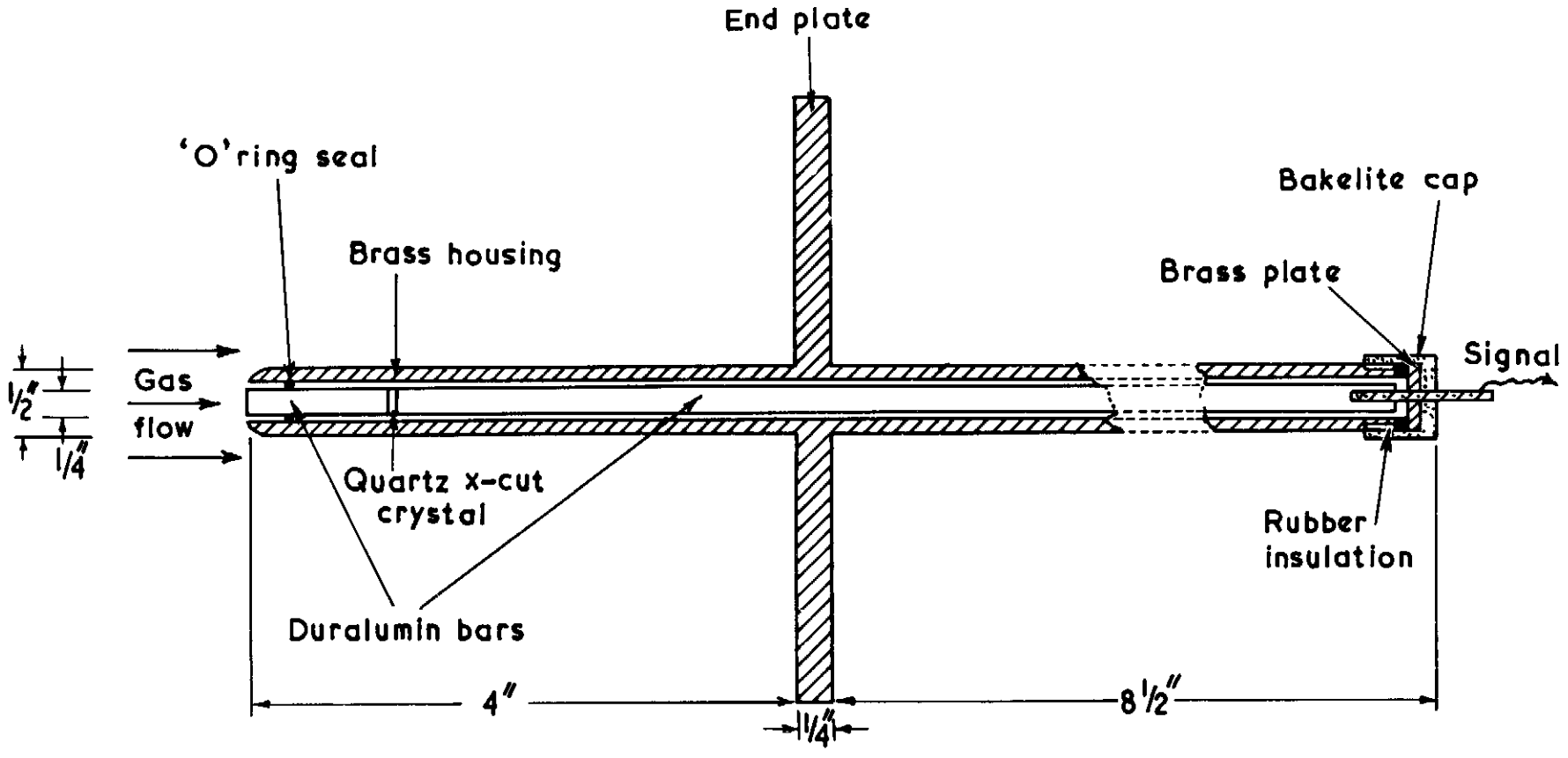

FIG. 1

Stagnation point pressure probe

FIG. 2

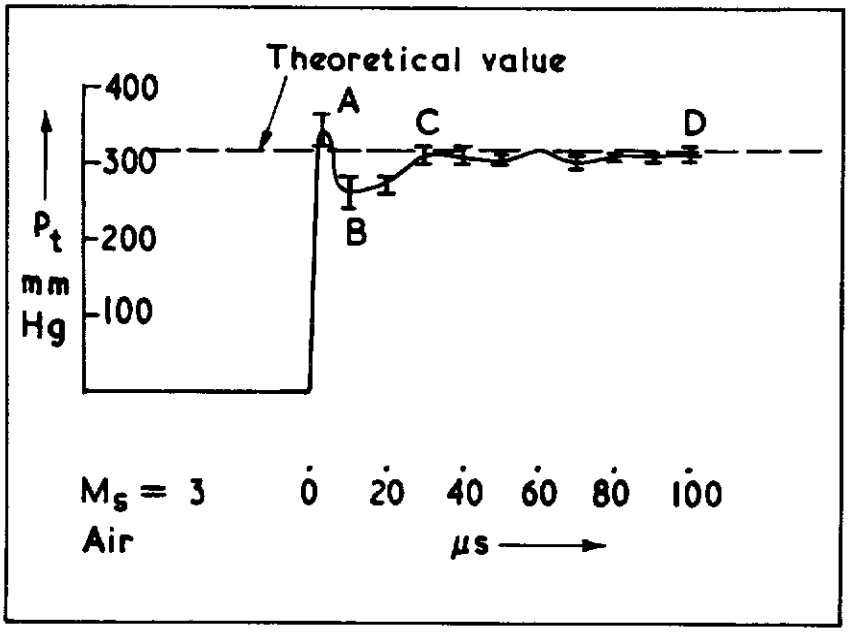
Theoretical value
400
300
200
100
P_t
mm
Hg
A
B
C
D
$M_s = 3$
Air
0
20
40
60
80
100
μs

FIG. 3

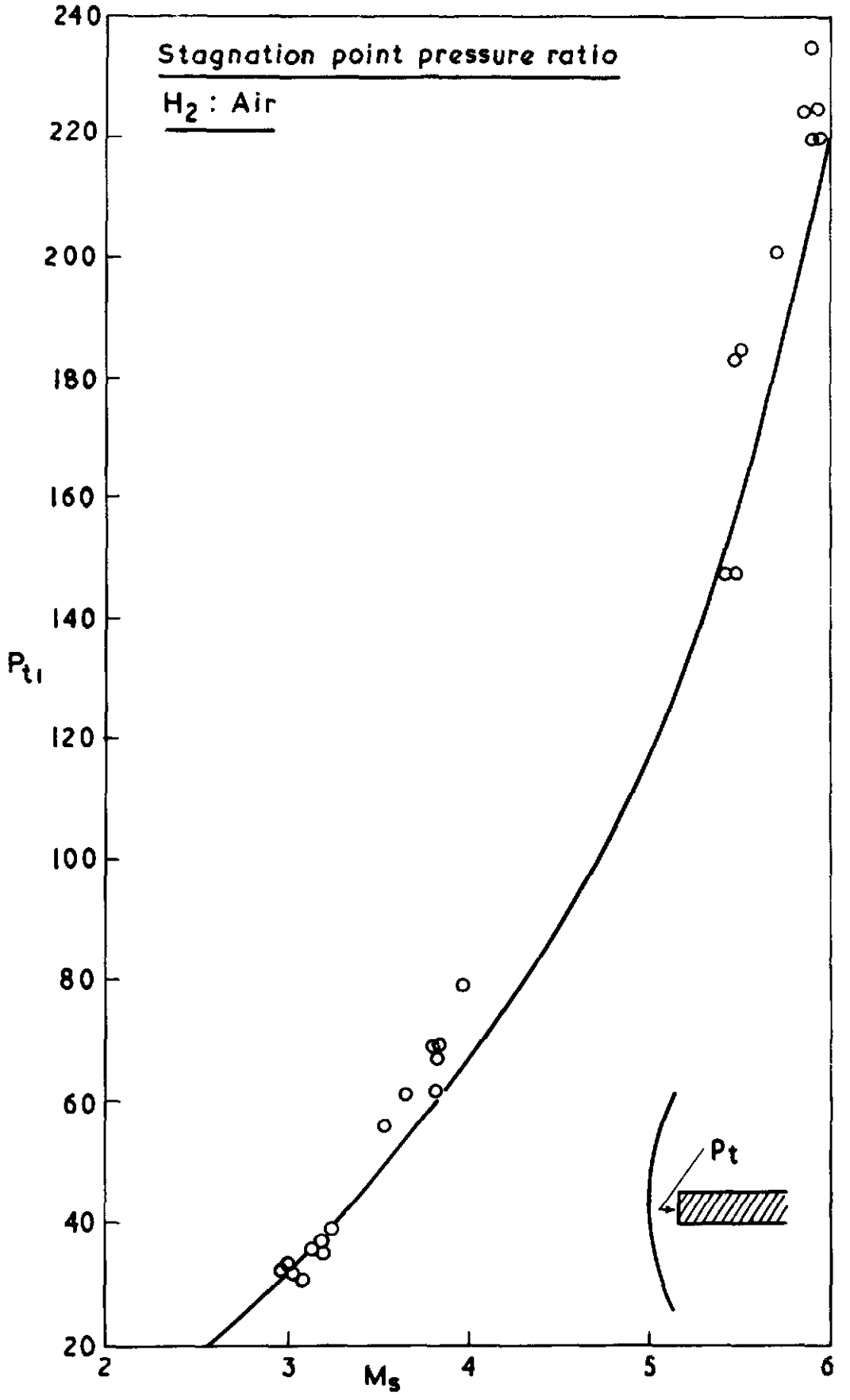
Stagnation point pressure ratio
H2 : Air
Pt1
Ms
Pt
240
220
200
180
160
140
120
100
80
60
40
20
2
3
4
5
6

FIG. 6

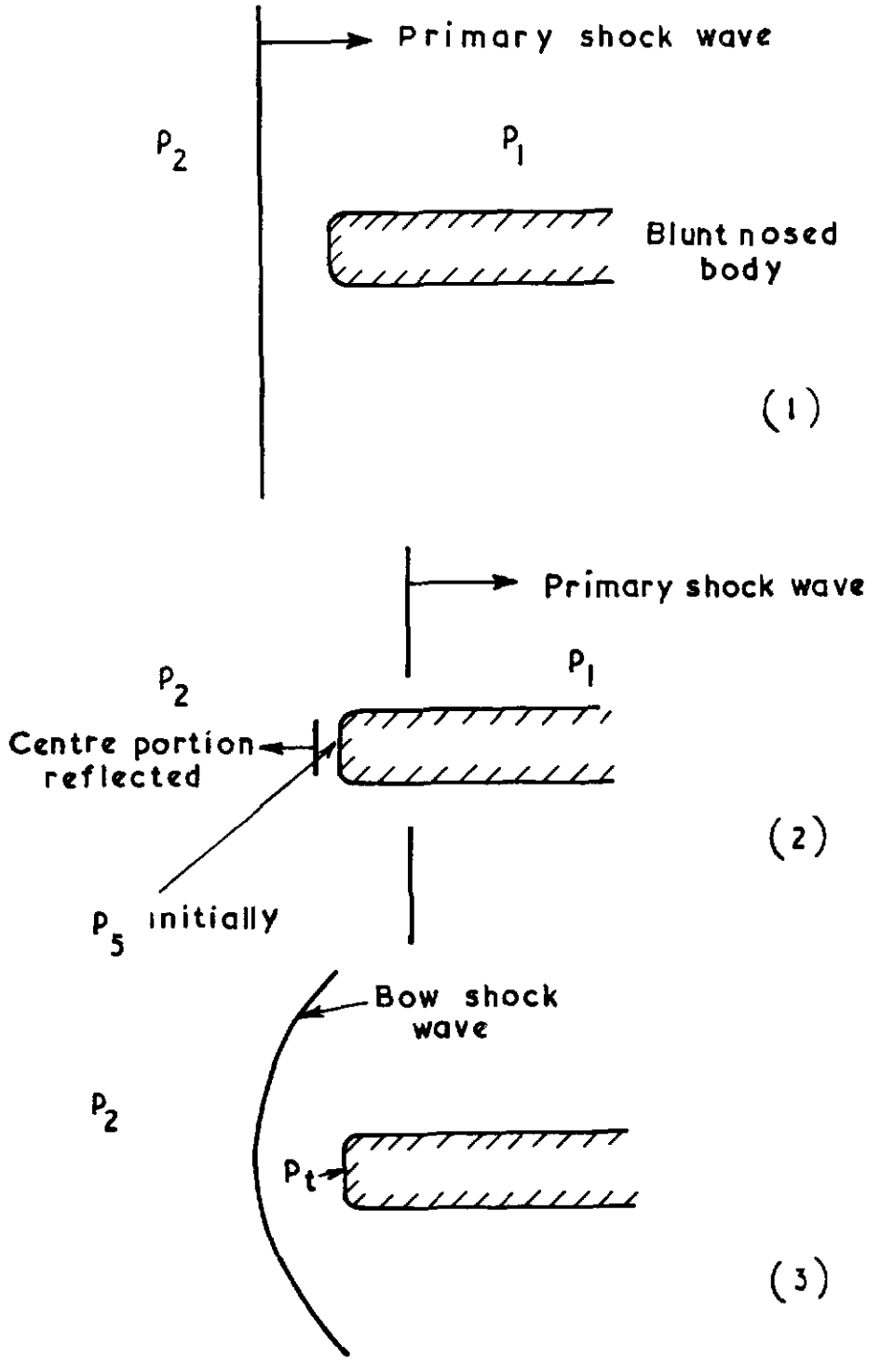

Bow shock establishment model

FIG.7.

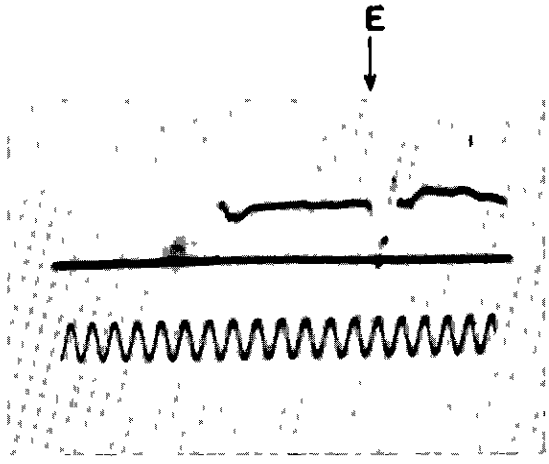

Air

M_s = 2·5

p_1 = 20 cms Hg

Timing trace 50Kc/s

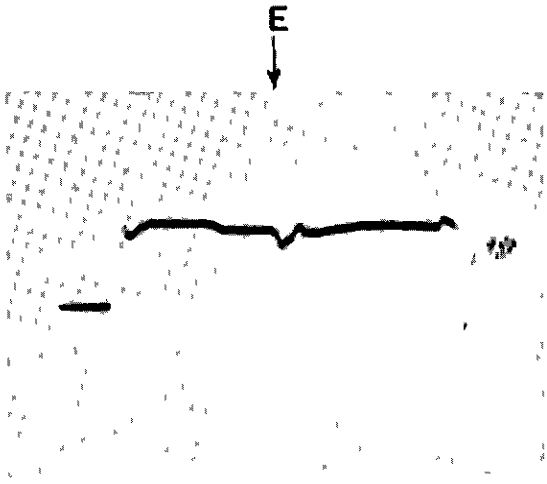

Oxygen

M_s = 2·5

p_1 = 20 cms Hg

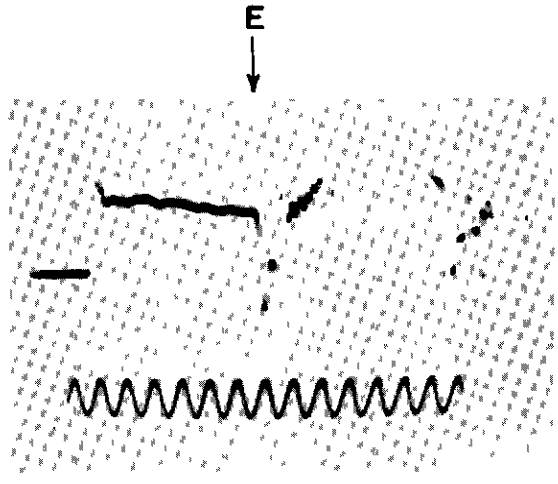

Argon

M_s = 2·5

p_1 = 20 cms Hg

Timing trace 50Kc/s

Stagnation point pressure - time profiles for air oxygen and argon.

E = end of recording time for the pressure bar gauge.

FIG.8

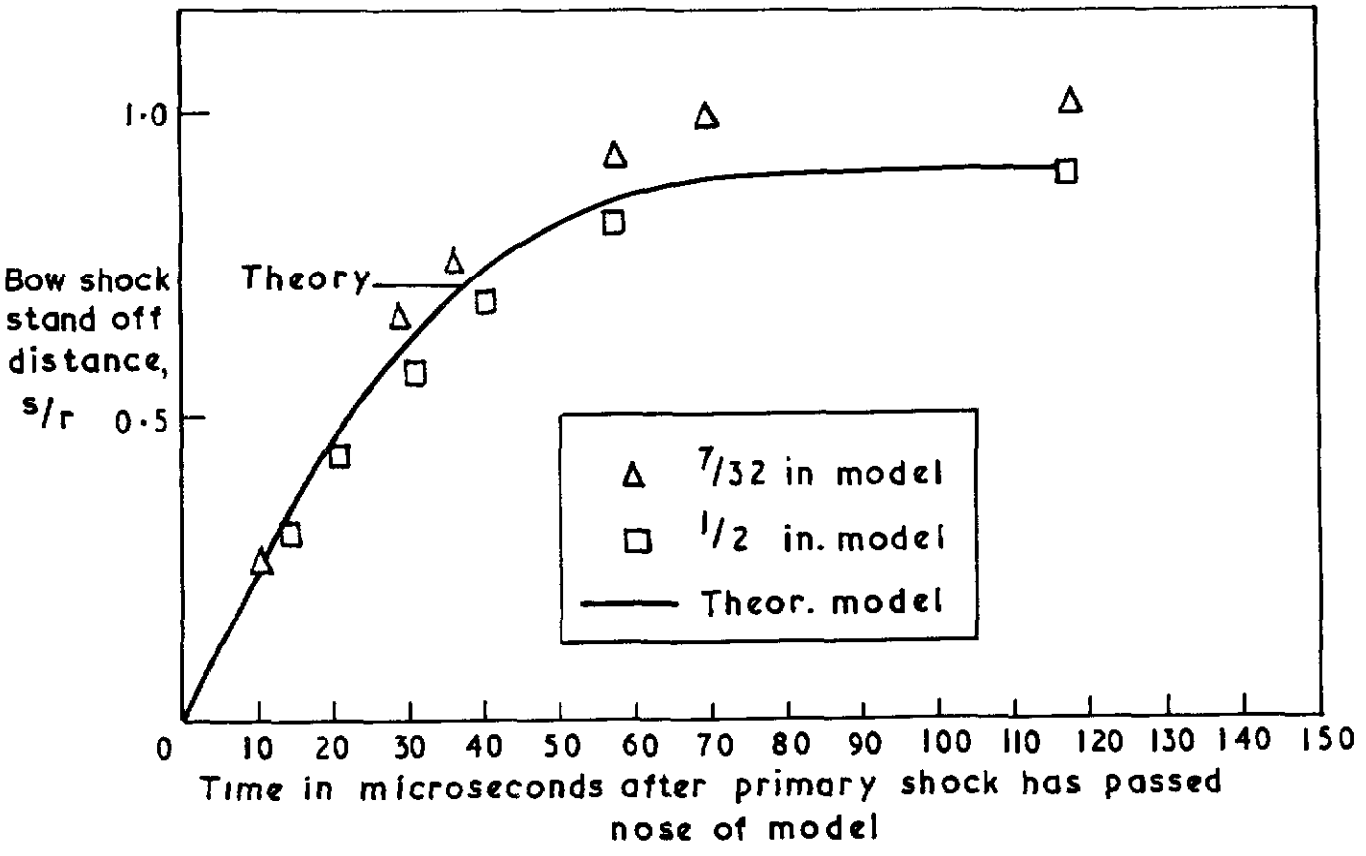

N_2: air. 1/2 in. and 7/32 in. diameter models. $M_s = 2 \cdot 23$, $p_1 = 50$ mm Hg.

FIG. 9

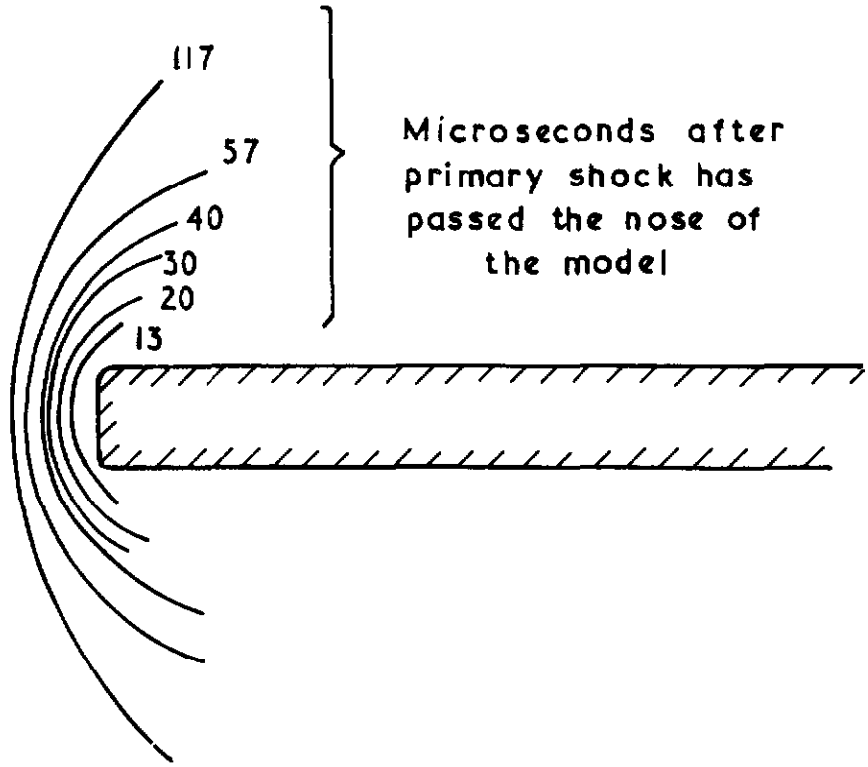

Build up of bow shock wave at the nose of a blunt body. 1/2 in. model. $M_s = 2{\cdot}23$

FIG. 10 (a)

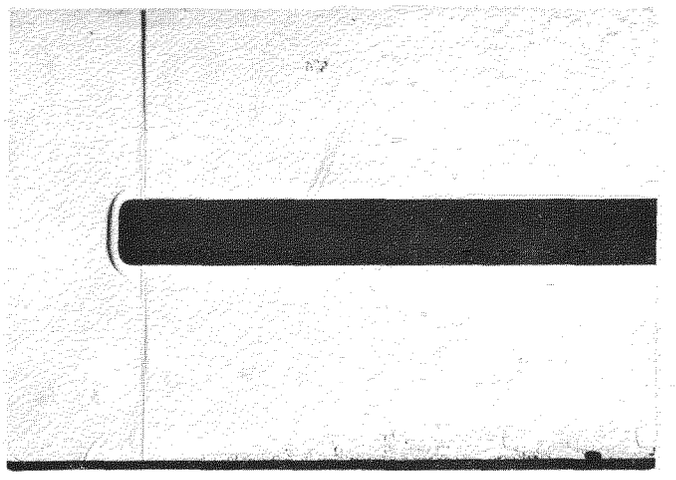

Bow shock establishment

1/2 in. diameter model

$M_s = 2.23$

Time after primary shock has passed nose of model.

10 μs

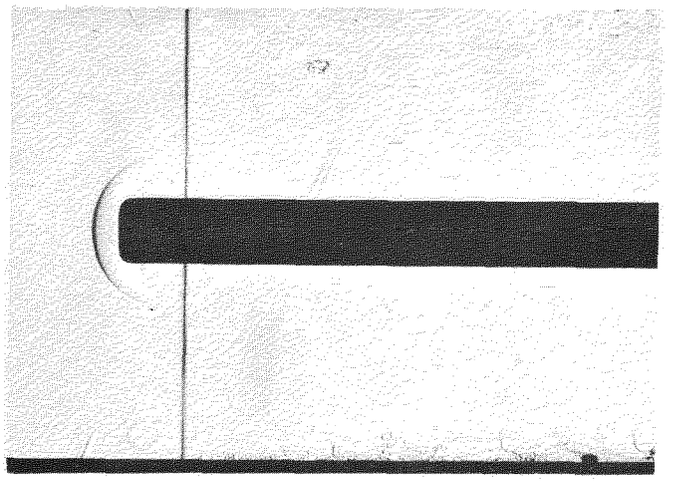

30 μs

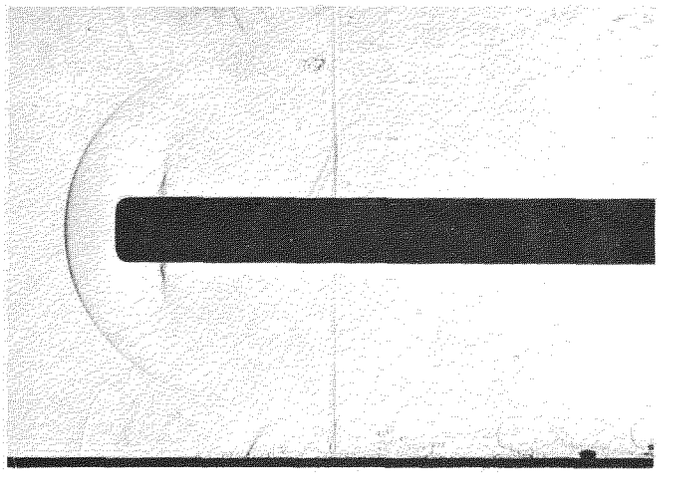

57 μs

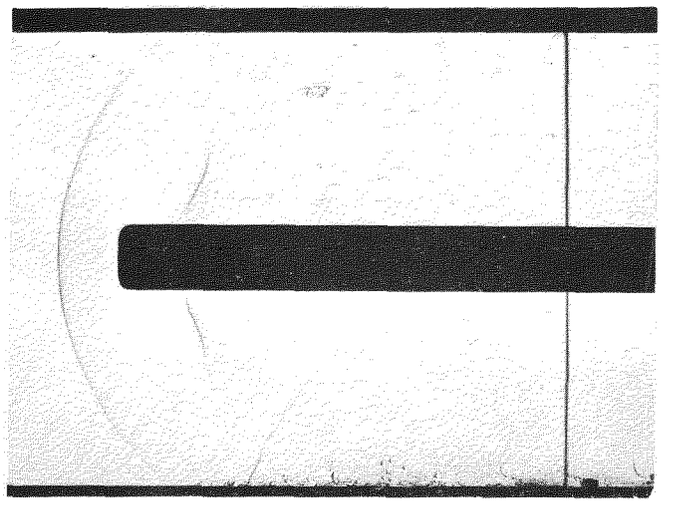

117 μs

FIG 10 (b)

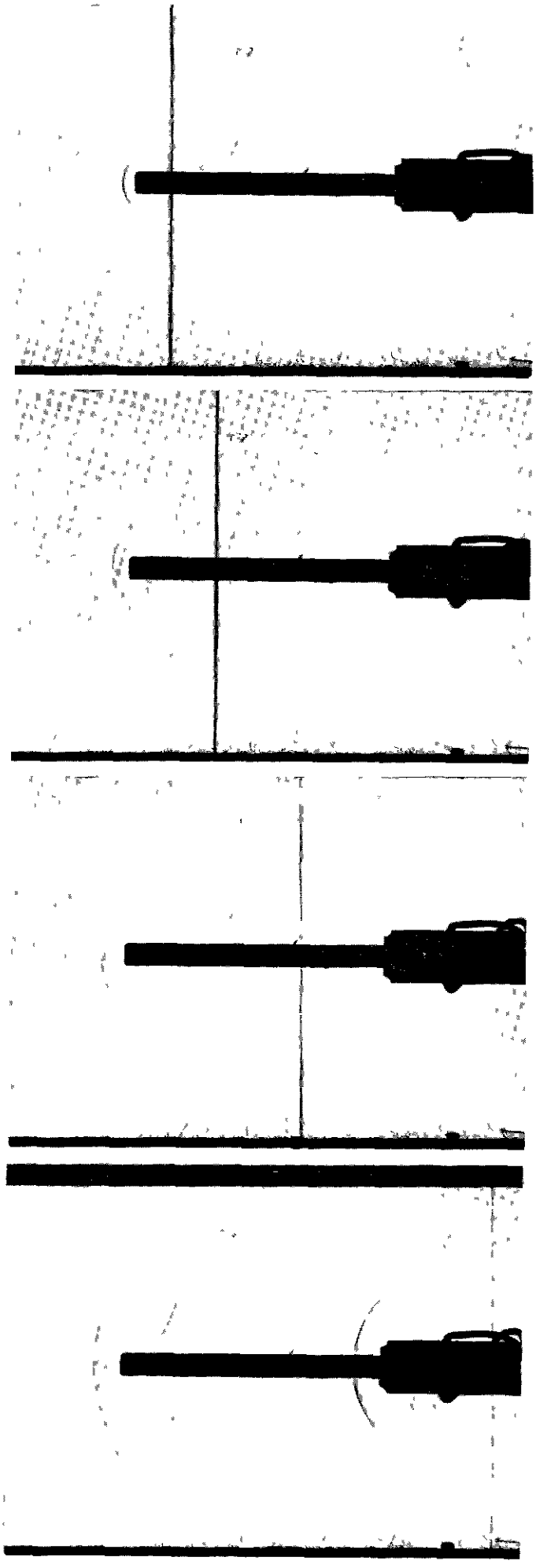

Bow shock establishment

7/32 in diameter model

$M_S = 2{\cdot}23$

Time after primary shock has passed nose of model

20 μs

46 μs

80 μs

120 μs

A.R.C. C.P. No.776
Davies, L.

A shock-tube study has been made of the bow shock establishment process in air and the pressure-time profiles at the stagnation point of a blunt-nosed body in air, oxygen and argon during the establishment of supersonic flow conditions over the body. Incident shock Mach number range 2 → 8.

A.R.C. C.P. No.776
Davies, L.

A shock-tube study has been made of the bow shock establishment process in air and the pressure-time profiles at the stagnation point of a blunt-nosed body in air, oxygen and argon during the establishment of supersonic flow conditions over the body. Incident shock Mach number range 2 → 8.

A.R.C. C.P. No.776
Davies, L.

A shock-tube study has been made of the bow shock establishment process in air and the pressure-time profiles at the stagnation point of a blunt-nosed body in air, oxygen and argon during the establishment of supersonic flow conditions over the body. Incident shock Mach number range 2 → 8.

Printed and published by
HER MAJESTY'S STATIONERY OFFICE
To be purchased from
York House, Kingsway, London W C.2
423 Oxford Street, London W 1
13A Castle Street, Edinburgh 2
109 St Mary Street, Cardiff
39 King Street, Manchester 2
50 Fairfax Street, Bristol 1
35 Smallbrook, Ringway, Birmingham 5
80 Chichester Street, Belfast 1
or through any bookseller

Printed in England

S.O. Code No. 23-9015-76